New physics in single-top production

Oliver Maria Kind for the CDF, CMS, D0 and ATLAS Collaborations

Institut für Physik, Humboldt-Universität zu Berlin, Newtonstraße 15, 12489 Berlin, Germany

DOI: http://dx.doi.org/10.3204/DESY-PROC-2014-02/33

In this paper an overview of recent results on the search for physics beyond the Standard Model in the electro-weak top-quark production from the ATLAS, D0, CDF and CMS collaborations is given. This includes searches for W' and b^* resonances as well as measurements of *CP* violation, the W helicity fractions and the top-quark polarisation in single-top production. A brief review on the search for flavour-changing neutral currents and cross-section measurements with respect to the CKM matrix element V_{tb} is given.

1 Introduction

The electro-weak production of top-quarks (single-top) provides a unique window for searches of new physics beyond the Standard Model (SM). Effects of new physics can manifest themselves either as new resonances in the production process or alter the structure or strength of the weak coupling of the top-quark. This would result in visible mass peaks in the measurement or in deviations of the observed cross-sections from the SM prediction. Experimentally, such effects are studied best in single-top production for which the cross-section is directly proportional to the weak coupling of the top-quark. This is different for the more dominant $t\bar{t}$ production process. In top-quark pair production, any modification of the weak coupling would alter only the branching fractions of the top-quark decay which are not measurable at a hadron collider. Another advantage of single-top production is that the scale for new physics, Λ_{NP}, can be probed at higher energies. The contribution of new physics to single-top production would scale as $(\sqrt{s}/\Lambda_{NP})^n$, while for top-pair production its contribution is only $(m_t/\Lambda_{NP})^n$ with n being the dimension in the effective operator framework and $\sqrt{s}$ denoting the centre-of-mass energy of the hard scattering process. The latter can be substantially larger than the mass of the top-quark, m_t, at the Tevatron or the LHC [1, 2].

Modifications of the Wtb vertex by new physics can be described by an effective Lagrangian using so-called anomalous couplings

$$\mathcal{L} = -\frac{g}{\sqrt{2}}\bar{b}\gamma^\mu \left(V_L P_L + V_R P_R\right) t W^-_\mu - \frac{g}{\sqrt{2}}\bar{b}\frac{i\sigma^{\mu\nu}}{m_W} q_\nu \left(g_L P_L + g_R P_R\right) t W^-_\mu + \text{h.c.} \qquad (1)$$

with the projection operators $P_{L,R} = \frac{1}{2}(1 \mp \gamma^5)$ and the four-momentum transfer q at the Wtb vertex. The anomalous couplings V_L, V_R, g_L and g_R are all complex and vanish in the SM, except for V_L which is real and equal to V_{tb}.

In the SM three production channels exist. These are the production in the t and s-channel, and the associated production of a W boson and a top-quark, as shown in Fig. 1. For all three channels cross-section calculations are available at next-to-leading order (NLO) QCD [3, 4, 5].

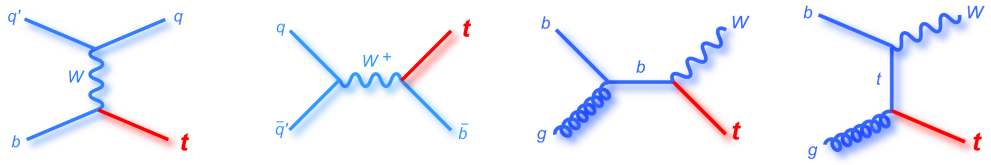

(a) t-channel (b) s-channel (c) Associated Wt production

Figure 1: Feynman diagrams of single-top production at leading-order QCD in the SM. Three production channels exist: the exchange of a W in the t-channel (a), s-channel production (b) and the associated production of a W boson (c).

Single-top production was first observed at the Tevatron [6, 7] in the t and s-channel and later also at the LHC [8, 9, 10, 11] in the t and Wt channels. All results are consistent with the SM prediction.

2 W′ Searches

Charged massive vector gauge bosons, W′, are proposed by several extensions of the SM, such as warped extra-dimensions [12, 13, 14], technicolour models [15, 16], right-handed massive W bosons [17] or little higgs theories [18, 19]. As indicated in Fig. 2, the final-state of the W′ decay is the same as for the s-channel production in the SM. The motivation to choose the $W' \to tb \to \ell\nu bb$ channel is two-fold: many models propose large couplings to the third generation of quarks which also disfavour the all-hadronic searches, and moreover, searches for leptonic decays of the W′ have a lower sensitivity to the lepto-phobic W′ models. In order to perform model-independent tests, one defines an effective Lagrangian containing left and right-handed couplings of the W′

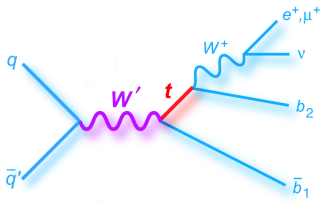

Figure 2: W′ production at tree-level. Besides the $W' \to t\bar{b}$ process shown, the process $W' \to \bar{t}b$ also exists.

$$\mathcal{L} = \frac{V'_{ij}}{2\sqrt{2}} \bar{f}_i \gamma_\mu \left(g'_{\mathrm{R}ij}(1+\gamma^5) + g'_{\mathrm{L}ij}(1-\gamma^5) \right) W'^{\mu} f_j + h.c. \tag{2}$$

with the left-handed and right-handed couplings g'_{L}, g'_{R} and V' denoting the CKM matrix element in the case of quarks and δ_{ij} for leptons. For right-handed couplings the situation is more complex since the mass of the right-handed neutrino involved in the process is not known. For small masses of the right-handed neutrino, hadronic and leptonic decays are allowed, while for masses larger than the W′ mass only hadronic decays are allowed. The left-handed W′ (W'_{L}) can decay leptonically or hadronically, however, for the leptonic decay, the final-state is the same as for SM s-channel production causing an interference. A common choice for the couplings are the two pure cases, W'_{L} with $g_{\mathrm{L}} = g_{\mathrm{w}}$, $g_{\mathrm{R}} = 0$ and the right-handed W′ (W'_{R}) with $g_{\mathrm{L}} = 0$, $g_{\mathrm{R}} = g_{\mathrm{w}}$, and the mixed case with $g_{\mathrm{L}} = g_{\mathrm{w}}$, $g_{\mathrm{R}} = g_{\mathrm{w}}$.

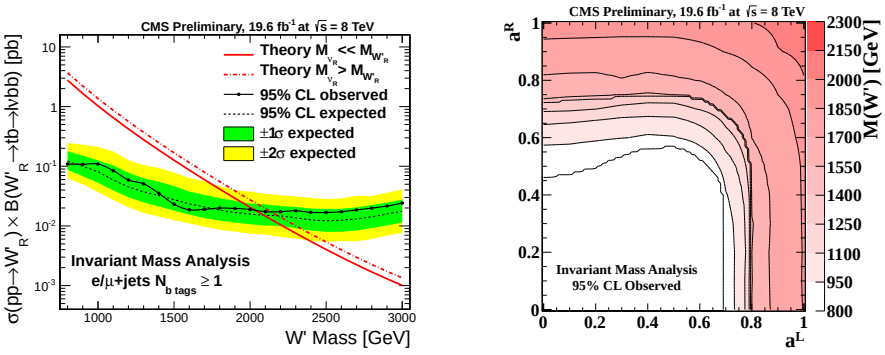

(a) Cross-section limits (b) Coupling strength contour

Figure 3: The left-hand figure (a) shows the upper limit on the production cross-section for W'_R times the branching ratio dependent on the W' mass. The contour plot on the right (b) shows the lower limit of the W' mass dependent on the coupling strengths a_L and a_R. Both figures are taken from [20].

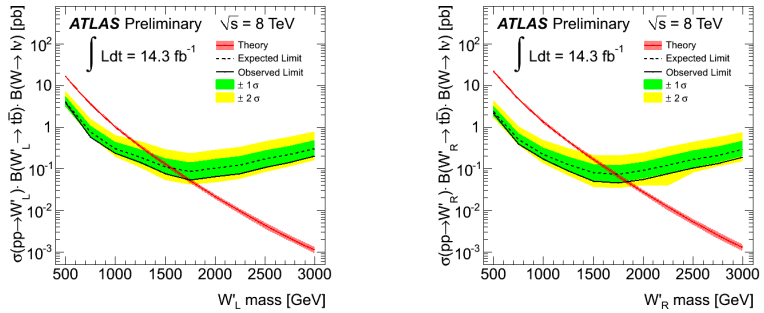

(a) Cross-section limits, W'_L (b) Cross-section limits, W'_R

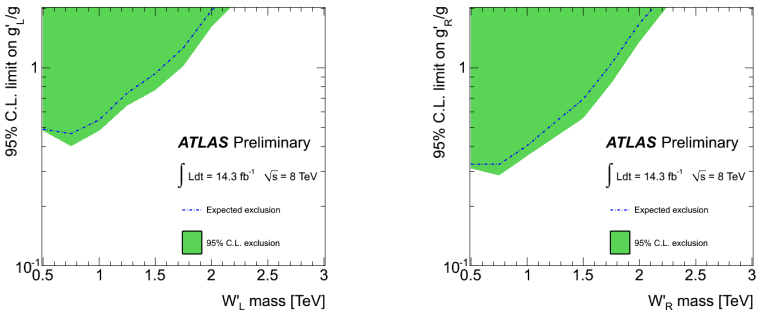

(c) Exclusion limits, W'_L (d) Exclusion limits, W'_R

Figure 4: The upper figures show the upper limit on the production cross-section times branching ratio for the W'_L (a) and W'_R (b). The red lines indicate the predictions for the case $m(\nu_R) > m(W')$. In figures (c) and (d) the exclusion limits for the left and right-handed cases are presented dependent on the coupling strength and the W' mass. All figures are taken from [21].

2.1 W′ Search at CMS

The CMS collaboration analysed 19.6 /fb of the 2012 data-set with a centre-of-mass energy of 8 TeV [20]. A cut-based analysis was performed using a typical event selection for the single-top s-channel by requiring one isolated high-$p_\perp$ electron or muon, at least two high-$p_\perp$ jets, at least one of them b-tagged and a significant amount of missing transverse energy. The top-quark was reconstructed by imposing a W mass constraint. The analysis results are collected in Fig. 3. Upper limits of the W′ production cross-section have been determined, dependent on the W′ mass, using multiple predictions for the signal in the range of 0.8 – 3 TeV, as shown in Fig. 3a. The signal was generated for the two scenarios of the right-handed neutrino mass, while neglecting the SM s-channel interference. A comparison of the cross-section limits with the prediction indicated by the red lines yields a lower limit for the mass of the W'_R (and W'_L when ignoring the interference with SM s-channel) of $m(\mathrm{W}') > 2.03$ TeV@95% C.L. In addition, mass limits were determined by varying the coupling strengths $a_{\mathrm{L,R}} = g_{\mathrm{L,R}}/g_\mathrm{w}$ in the range between 0 and 1 resulting in Fig. 3b.

2.2 W′ Search at ATLAS

For the W′ search at ATLAS an integrated luminosity of 14.3 /fb of the 8 TeV data was analysed [21]. Instead of a simple cut-based analysis, boosted decision trees with 14 input variables were used for the signal extraction. Only the scenario with the mass of the right-handed neutrino larger than the W'_R mass was studied. As for the CMS analysis, the interference with the SM s-channel production was neglected in the case of the W'_L. Figure 4 presents the main analysis results. From the upper limits of the production cross-sections lower mass limits for W'_L and W'_R are obtained: $m(\mathrm{W}'_\mathrm{L}) > 1.74$ TeV and $m(\mathrm{W}'_\mathrm{R}) > 1.84$ TeV, both at 95% C.L. Exclusion limits of the left and right-handed coupling strengths $g_{\mathrm{L,R}}/g_\mathrm{w}$ versus the W′ mass are also shown. In contrast to the CMS analysis the coupling strengths had been varied separately and their range was extended to values of 2.

3 b* Searches

The ATLAS collaboration has published final results on searches for single b* production using an integrated luminosity of 4.7 /fb at $\sqrt{s} = 7$ TeV [22]. In this search the b* resonance decays into a W boson and a single top-quark as described in [23]. These kinds of couplings to the third generation of SM quarks occur in some Randal–Sundrum models [24, 25] or composite Higgs models [26, 27, 28]. As for the W′ searches, the b* interaction is described by using effective Lagrangians for the production and decay of the b*. They contain the left and right-handed couplings κ_L, κ_R for the b* production, and g_L, g_R for its decay. The analysis was performed for the case of

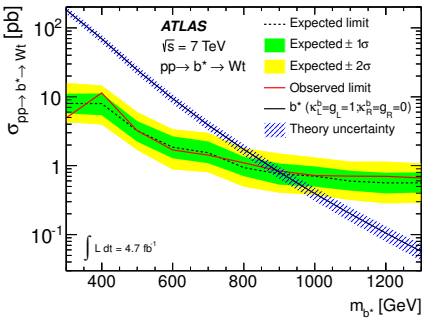

Figure 5: Observed and expected upper cross-section limits for the left-handed b* production and decay at ATLAS [22]. The black line indicates the predicted cross-section.

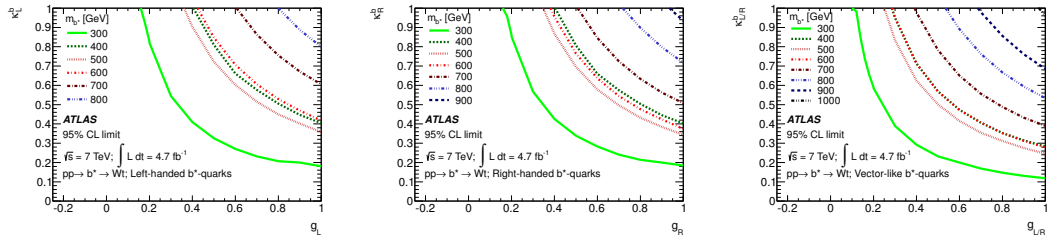

(a) Left-handed (b) Right-handed (c) Vector-like

Figure 6: Contours for several b^* lower mass limits in the two-dimensional plane of the couplings for the production and the decay of the b^*, for the case of left-handed (a), right-handed (b) and vector-like couplings (c). All figures are taken from [22].

both outgoing W bosons decaying leptonically ("di-lepton" channel) and one of them decaying hadronically ("lepton + jets" channel). The signal, which is very similar to the associated Wt production, was discriminated by using the scalar sum of the transverse momenta of all reconstructed objects, $H_\perp$, for the di-lepton case, and using the reconstructed invariant mass m^*_b for lepton + jets final-states. The resulting upper limit on the cross-section depending on the b^* mass and the corresponding prediction are presented in Fig. 5. The following lower mass limits are obtained:

pure left-handed	$\kappa_L = g_L = 1$	$m(b^*_L) > 870\,\text{GeV@95\% C.L.}$
pure right-handed	$\kappa_L = g_L = 0$	$m(b^*_R) > 920\,\text{GeV@95\% C.L.}$
mixed (vector-like)	$\kappa_L = g_L = 1$	$m(b^*_{L\|R}) > 1030\,\text{GeV@95\% C.L.}$

Mass contours in the plane of the left and right-handed couplings for the three cases are given in Fig. 6.

4 *CP* Violation

The violation of *CP* invariance is believed to be the reason for the matter-antimatter asymmetry in baryogenesis. However, the observed *CP* violation in the systems of neutral kaons and B-mesons can not fully account for the observed asymmetry. The ATLAS collaboration has performed a search for possible *CP* violation in single-top *t*-channel production at a centre-of-mass energy of $\sqrt{s} = 7\,\text{TeV}$ using an integrated luminosity of 4.66 /fb [29]. The decay of the top-quark can be described in the most general effective operator framework by an effective Lagrangian which contains left-handed and right-handed vector couplings, V_L and V_R, as well as tensor couplings g_L and g_R [30, 31]. While in the SM all couplings, except for $V_L = V_{tb}$, are supposed to be zero, a non-zero imaginary part

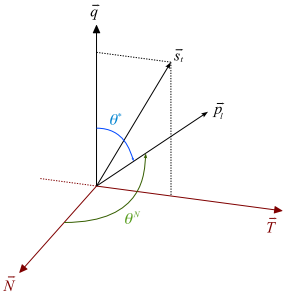

Figure 7: The angle θ^N is defined by the lepton momentum $\vec{p}^{\,\ell}$ and the direction $\vec{N}$ normal to the plane defined by the direction of the spectator quark $\vec{s}_t$ and the W boson, $\vec{q}$, in the rest-frame of the top-quark.

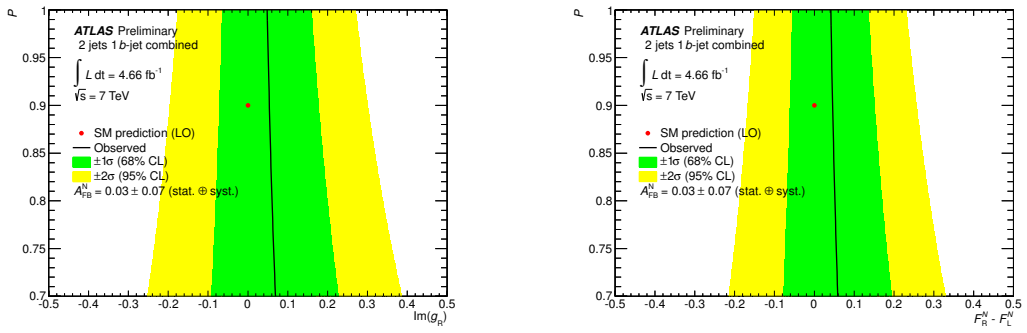

(a) Anomalous coupling $\Im(g_\mathrm{R})$

(b) Normal helicity fractions

Figure 8: The measurement of the forward-backward asymmetry A_FB^N allows to extract the imaginary part of the anomalous tensor coupling g_R for the top-quark decay depending on the polarisation $\mathcal{P}$ of the top-quark (a). The difference of the normal helicity fraction F_L^N and F_R^N of the W boson from the top-quark decay is also shown (b). Both figures are taken from [29].

of g_R would result in a violation of *CP* invariance. Since in the case of single-top t-channel production the top-quark is highly polarised ($\mathcal{P}\approx 0.9$) along the direction of the spectator quark, the forward-backward asymmetry A_FB^N of the angle θ^N, described in Fig. 7, is very sensitive to $\Im(g_\mathrm{R})$. While in the SM the value of A_FB^N is supposed to be zero, in the general case of non-zero anomalous couplings the relation $A_\mathrm{FB}^\mathrm{N} = 0.64\mathcal{P}\cdot\Im(g_\mathrm{R})$ holds. Here, $V_\mathrm{tb} = 1$ and $\Re(g_\mathrm{L}) = 0$ is assumed.

Using a standard single-top t-channel lepton + jets selection and applying an unfolding procedure for the distribution of event counts in bins of $\cos\theta^\mathrm{N}$ which takes migration effects into account, the ATLAS collaboration obtains $A_\mathrm{FB}^\mathrm{N} = 0.031 \pm 0.065(\mathrm{stat.})^{+0.029}_{-0.031}(\mathrm{syst.})$ for the forward-backward asymmetry. The resulting confidence intervals for the imaginary part of g_R depending on the degree of polarisation of the top-quark are depicted in Fig. 8a. Within its uncertainty this result is consistent with the SM expectation. The forward-backward asymmetry is also related to the W helicity fractions F_L^N and F_R^N, which are defined in the same basis as θ^N, by $A_\mathrm{FB}^\mathrm{N} = {}^3\!/_4\mathcal{P}\cdot(F_\mathrm{R}^\mathrm{N} - F_\mathrm{L}^\mathrm{N})$. In the SM the difference between F_L^N and F_R^N is zero. Figure 8b shows its confidence intervals for various values of the polarisation.

5 Helicity Fractions

The polarisation of the W boson in top-quark decays is sensitive to non-SM couplings of the Wtb vertex [32]. Since the W can be left-handed, right-handed or longitudinal, its total decay width splits into the corresponding partial widths, $\Gamma(\mathrm{t}\to\mathrm{Wtb}) = \Gamma_\mathrm{L} + \Gamma_\mathrm{R} + \Gamma_0$. The helicity fractions are defined as the branching ratios, hence $F_{\mathrm{L,R},0} = {}^{\Gamma_{\mathrm{L,R},0}}\!/_{\Gamma}$. Unitarity requires $F_\mathrm{L} + F_\mathrm{R} + F_0 = 1$. The latest SM predictions at QCD NNLO accuracy yield $F_\mathrm{L} = 0.311(5)$, $F_\mathrm{R} = 0.0017(1)$ and $F_0 = 0.687(5)$ [33]. In single-top events the helicity fractions can be obtained experimentally from the angular distribution of the angle θ_ℓ^* described in Fig. 7 between the lepton and the W

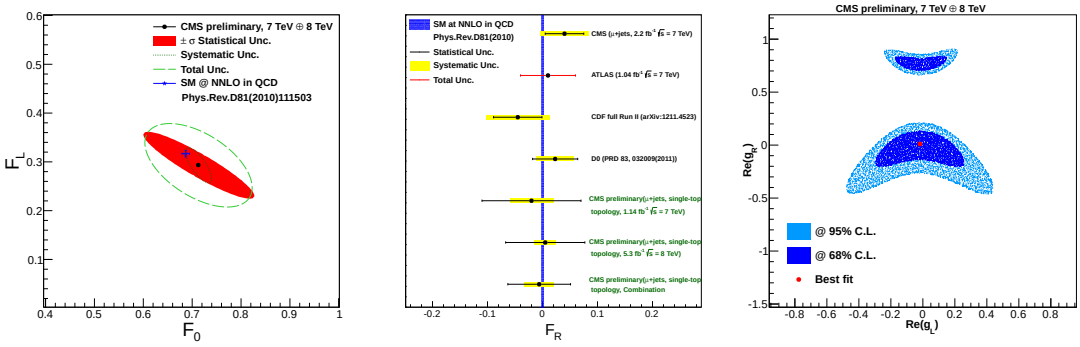

(a) F_{L} vs. F_0 (b) F_{R} measurements (c) Exclusion limits for g_{L} and g_{R}

Figure 9: In (a) the correlation of the measurements for the W helicity fractions F_{L} and F_0 is shown. The obtained value for F_{R} is indicated in (b) in comparison to other recent F_{R} measurements from the LHC and Tevatron experiments. The exclusion limits obtained from the measurement of the helicity fractions for the real part of the tensor couplings g_{L} and g_{R} are shown in (c). From [34].

boson

$$\frac{1}{\Gamma}\frac{\mathrm{d}\Gamma}{\mathrm{d}\cos\theta^*_\ell} = \tfrac{3}{8}\left(1-\cos\theta^*_\ell\right)^2 F_{\mathrm{L}} + \tfrac{3}{8}\left(1+\cos\theta^*_\ell\right)^2 F_{\mathrm{R}} - \tfrac{3}{4}\sin^2\theta^*_\ell F_0\,. \tag{3}$$

The measured helicity fractions can be used to constrain the anomalous couplings V_{L}, V_{R}, g_{L} and g_{R} at the Wtb decay vertex.

The CMS collaboration has released results on the W helicity fractions in single-top t-channel and s-channel events using an integrated luminosity of 1.14 /fb of the 7 TeV data-set and 4.66 /fb of the 8 TeV data-set in the μ + jets channel [34]. The helicity fractions F_{L} and F_0 have been used as fit parameters in a re-weighting procedure of all simulated events. A binned maximum likelihood fit of the simulated angular distributions to those in real data measured the following values: $F_{\mathrm{L}} = 0.293 \pm 0.069(\mathrm{stat.}) \pm 0.030(\mathrm{syst.})$ and $F_0 = 0.713 \pm 0.114(\mathrm{stat.}) \pm 0.023(\mathrm{syst.})$. Figure 9a shows these values together with their correlation. Assuming unitarity, a value of $F_{\mathrm{R}} = -0.006 \pm 0.057(\mathrm{stat.}) \pm 0.027(\mathrm{syst.})$ is obtained, which is contained in the overview of recent F_{R} measurements in Fig. 9b. All three measured helicity fractions are consistent with the SM prediction. The results have been used to set exclusion limits on the real parts of the anomalous tensor couplings g_{L} and g_{R} as presented in Fig. 9c. The best fit values are $g_{\mathrm{L}} = -0.014$ and $g_{\mathrm{R}} = 0.007$.

6 Top-Quark Polarisation in Single-Top Production

In single-top t-channel production the top-quarks are highly polarised because of the $V-A$ structure of the Wtb vertices. New physics beyond the SM would alter these couplings and affect the polarisation as shown in [30]. The degree of polarisation of the top-quark, $\mathcal{P}$, is related to the spin asymmetry by

$$A_\ell = \frac{N_\uparrow - N_\downarrow}{N_\uparrow + N_\downarrow} = \tfrac{1}{2}\mathcal{P}\cdot\alpha_\ell\,, \tag{4}$$

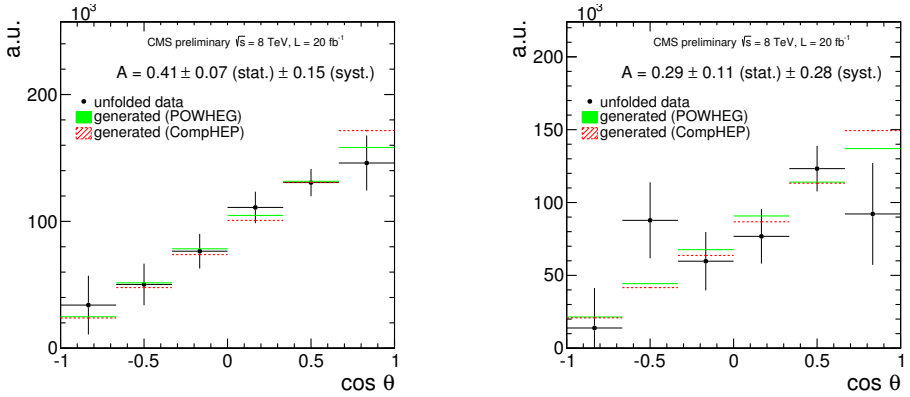

(a) Muon channel (b) Electron channel

Figure 10: Measured angular distributions of $\cos\theta_\ell^*$ for the muon channel (a) and electron channel (b) in single-top t-channel production (filled black circles). The results for two different generators are shown for comparison. Both figures are taken from [35].

where α_ℓ denotes the spin-analysing power, which is nearly one for charged leptons being used as spin analyser. Since the top-quark spin is preferably aligned along the direction of the recoil jet (spectator), the measurement is best performed by means of the angle θ_ℓ^*, which is defined here as the angle between the charged lepton from the top decay and the recoil jet in the rest-frame of the top-quark. The angular distribution of θ_ℓ^* in the top-quark decay is directly related to the spin asymmetry and thus to the polarisation

$$\frac{\mathrm{d}\Gamma}{\mathrm{d}\cos\theta_\ell^*} = \Gamma\left(\tfrac{1}{2} + A_\ell \cos\theta_\ell^*\right) = \tfrac{1}{2}\Gamma\left(1 + \mathcal{P}\alpha_\ell \cos\theta_\ell^*\right) . \tag{5}$$

The CMS collaboration has measured the top-quark polarisation in single-top t-channel production at $\sqrt{s} = 8\,\mathrm{TeV}$ using an integrated luminosity of $20\,/\mathrm{fb}$ [35]. After a common event selection for the lepton + jets channel, the signal was enhanced by using boosted decision trees. By means of a regularised unfolding method based on generalised matrix inversion [36], the angular distributions of the angle θ_ℓ^* were obtained for electrons and muons, as shown in Fig.10. The forward-backward asymmetry with respect to the angle θ_ℓ^* is a measure for the spin asymmetry A_ℓ. The resulting values are:

$$\begin{aligned} \text{electron channel} \quad & A_\mathrm{e} = 0.41 \pm 0.07\,(\text{stat.}) \pm 0.15\,(\text{syst.}) \\ \text{muon channel} \quad & A_\mu = 0.29 \pm 0.11\,(\text{stat.}) \pm 0.28\,(\text{syst.}) \\ \text{combined} \quad & A_\ell = 0.41 \pm 0.06\,(\text{stat.}) \pm 0.16\,(\text{syst.}) \end{aligned}$$

The combined result is connected to a polarisation of the top-quark in single-top t-channel production of $\mathcal{P} = 0.82 \pm 0.12(\text{stat.}) \pm 0.32(\text{syst.})$.

7 Cross-Section Measurements

Combined measurements of the different single-top production channels also provide a good way to search for new physics beyond the SM. The DØ collaboration recently reported evidence for single-top production in the s-channel with a significance of 3.7 standard deviations

in proton-antiproton collisions at a centre-of-mass energy of 1.96 TeV using an integrated luminosity of 9.7 /fb [38]. The analysis, which was a combination of artificial neural networks, boosted decision trees and matrix elements methods, includes independent measurements of the t-channel and s-channel cross-sections. The results are shown in Fig. 11 in comparison with the prediction of the SM and those of several other models. The measurements are, however, not yet precise enough to distinguish between the predictions of the different models.

The CKM matrix element V_{tb}, which plays a key role in searches for new physics, is directly accessible from single-top cross-section measurements by using the relation $|V_{\mathrm{tb}}|^2_{\mathrm{obs}} = \frac{\sigma_{\mathrm{obs}}}{\sigma_{\mathrm{SM}}} \cdot |V_{\mathrm{tb}}|^2_{\mathrm{SM}}$. In the SM $|V_{\mathrm{tb}}|_{\mathrm{SM}} \approx 1$and the following assumptions are used: $|V_{\mathrm{tb}}|^2 \gg |V_{\mathrm{ts}}|^2 + |V_{\mathrm{td}}|^2$ and the Wtb vertex is of $V-A$ type while CP is conserved. Two scenarios are usually looked at: in one scenario anomalous left-handed couplings f_1^{L} are allowed such that values of $|V_{\mathrm{tb}} \cdot f_1^{\mathrm{L}}| > 1$ are possible, while in the other $|V_{\mathrm{tb}}|$ is restricted to the SM region of 0 to 1 with $f_1^{\mathrm{L}} = 1$. Recent results for the two scenarios by the Tevatron and LHC experiments are collected in Tab. 1. All values are consistent with the SM.

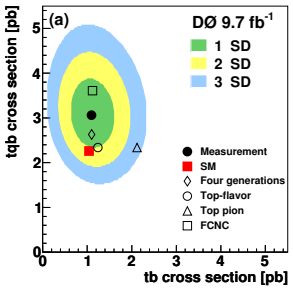

Figure 11: Single-top cross-section measurements for the t and s-channel by the DØ collaboration [38]. The predictions of the SM and several other models are indicated in the figure.

Experiment	Process	$\int dL$ [fb]	$\lvert V_{\mathrm{tb}} \cdot f_1^{\mathrm{L}} \rvert$	$\lvert V_{\mathrm{tb}} \rvert$@95% C.L.	Published	
CDF	$s+t$	7.5	0.96 ± 0.10	>0.78	Apr 12	[39]
DØ	$s+t$	9.7	$1.12^{+0.09}_{-0.08}$	>0.92	Jun 13	[38]
CMS	t	5.0	0.96 ± 0.08	>0.81	Sep 12	[40]
CMS	Wt	12.2	1.03 ± 0.13	>0.78	Jul 13	[41]
ATLAS	t	5.8	$1.04^{+0.10}_{-0.11}$	>0.80	Sep 12	[42]

Table 1: Recent results on V_{tb} by single-top measurements from the Tevatron and LHC experiments.

8 Summary

Single-top signatures allow many models of new physics to be tested. Several new results from the LHC and Tevatron experiments are available which are summarised in this paper. Searches for W' and b^* resonances conducted by ATLAS and CMS did not reveal any signal. Also, the ATLAS collaboration found no indication for CP violation in the single-top sector. The CMS collaboration measured the W boson helicity fractions and the top-quark polarisation in single-top events for the first time. No evidence for flavour-changing neutral currents was seen by ATLAS and CMS (this topic is discussed in [43] and references therein). All recent cross-section and V_{tb} measurements are consistent with the SM within their uncertainties.

References

[1] T. M. P. Tait and C. -P. Yuan, Phys. Rev. D **63** (2000) 014018, hep-ph/0007298.

[2] Q. -H. Cao, J. Wudka and C. -P. Yuan, Phys. Lett. B **658** (2007) 50, arXiv:0704.2809 [hep-ph].

[3] G. Bordes and B. van Eijk, Nucl. Phys. B **435** (1995) 23.

[4] T. Stelzer, Z. Sullivan and S. Willenbrock, Phys. Rev. D **56** (1997) 5919, hep-ph/9705398.

[5] T. Stelzer, Z. Sullivan and S. Willenbrock, Phys. Rev. D **58** (1998) 094021, hep-ph/9807340.

[6] CDF Collaboration, Phys. Rev. Lett. **103** (2009) 092002, arXiv:0903.0885 [hep-ex].

[7] DØ Collaboration, Phys. Rev. Lett. **103** (2009) 092001, arXiv:0903.0850 [hep-ex].

[8] ATLAS Collaboration, Phys. Lett. B **717** (2012) 330 arXiv:1205.3130 [hep-ex].

[9] CMS Collaboration, JHEP **1212** (2012) 035, arXiv:1209.4533 [hep-ex].

[10] ATLAS Collaboration, Phys. Lett. B **716** (2012) 142, arXiv:1205.5764 [hep-ex].

[11] CMS Collaboration, Phys. Rev. Lett. **110** (2013) 022003, arXiv:1209.3489 [hep-ex].

[12] G. Burdman, B. A. Dobrescu and E. Ponton, Phys. Rev. D **74** (2006) 075008, hep-ph/0601186.

[13] T. Appelquist, H. -C. Cheng and B. A. Dobrescu, Phys. Rev. D **64** (2001) 035002, hep-ph/0012100.

[14] H. -C. Cheng, C. T. Hill, S. Pokorski and J. Wang, Phys. Rev. D **64** (2001) 065007, hep-th/0104179.

[15] E. Malkawi, T. M. P. Tait and C. P. Yuan, Phys. Lett. B **385** (1996) 304, hep-ph/9603349.

[16] R. S. Chivukula and E. H. Simmons and J. Terning, Phys. Rev. D **53** (1996) 5258.

[17] J. C. Pati and A. Salam, Phys. Rev. D **10** (1974) 275 [Erratum-ibid. D **11** (1975) 703].

[18] M. Perelstein, Prog. Part. Nucl. Phys. **58** (2007) 247, hep-ph/0512128.

[19] M. Schmaltz and D. Tucker-Smith, Ann. Rev. Nucl. Part. Sci. **55** (2005) 229, hep-ph/0502182.

[20] CMS Collaboration, CMS-PAS-B2G-12-010.

[21] ATLAS Collaboration, ATLAS-CONF-2013-050.

[22] ATLAS Collaboration, Phys. Lett. B **721** (2013) 171, arXiv:1301.1583 [hep-ex].

[23] J. Nutter, R. Schwienhorst, D. G. E. Walker and J. -H. Yu, Phys. Rev. D **86** (2012) 094006, arXiv:1207.5179 [hep-ph].

[24] C. Cheung, A. L. Fitzpatrick and L. Randall, JHEP **0801** (2008) 069, arXiv:0711.4421 [hep-th].

[25] A. L. Fitzpatrick, G. Perez and L. Randall, Phys. Rev. Lett. **100** (2008) 171604, arXiv:0710.1869 [hep-ph].

[26] C. Bini, R. Contino and N. Vignaroli, JHEP **1201** (2012) 157, arXiv:1110.6058 [hep-ph].

[27] N. Vignaroli, JHEP **1207** (2012) 158, arXiv:1204.0468 [hep-ph].

[28] N. Vignaroli, Phys. Rev. D **86** (2012) 115011, arXiv:1204.0478 [hep-ph].

[29] ATLAS Collaboration, ATLAS-CONF-2013-032.

[30] J. A. Aguilar-Saavedra, Nucl. Phys. B **812** (2009) 181, arXiv:0811.3842 [hep-ph].

[31] J. A. Aguilar-Saavedra, Nucl. Phys. B **821** (2009) 215, arXiv:0904.2387 [hep-ph].

[32] J. A. Aguilar-Saavedra, J. Carvalho, N. F. Castro, F. Veloso and A. Onofre, Eur. Phys. J. C **50** (2007) 519, hep-ph/0605190.

[33] A. Czarnecki, J. G. Korner and J. H. Piclum, Phys. Rev. D **81** (2010) 111503, arXiv:1005.2625 [hep-ph].

[34] CMS Collaboration, CMS-PAS-TOP-12-020.

[35] CMS Collaboration, CMS-PAS-TOP-13-001.

[36] V. Blobel, hep-ex/0208022.

[37] ATLAS Collaboration, Phys. Lett. B **712** (2012) 351, arXiv:1203.0529 [hep-ex].

[38] V. M. Abazov *et al.* [D0 Collaboration], Phys. Lett. B **726** (2013) 656, arXiv:1307.0731 [hep-ex].

[39] CDF Collaboration, CDF Conference Note 10793.

[40] CMS Collaboration, CMS-PAS-TOP-12-011.

[41] CMS Collaboration, CMS-PAS-TOP-12-040.

[42] ATLAS Collaboration, ATLAS-CONF-2012-132.

[43] E. Yazgan, these proceedings.